SDSS'Rio 2010 STABILITY AND DUCTILITY OF STEEL STRUCTURES
E. Batista, P. Vellasco, L. de Lima (Eds.)
Rio de Janeiro, Brazil, September 8 - 10, 2010

ELASTO-PLASTIC BUCKLING BEHAVIOR OF H-SHAPED BEAM WITH LARGE DEPTH-THICKNESS RATIO UNDER CYCLIC LOADING

Tao WANG*, Kikuo IKARASHI*

* Department of Architecture and building Engineering, Tokyo Institute of Technology
e-mails: wanntao2@gmail1.com, ikarasahi@arch.titech.ac.jp

Keywords: Coupled Buckling, Vertical Buckling, Plate Slenderness ratio, Plastic Deformation Capacity.

Abstract. *Plastic deformation capacity of thin-walled structure is not only affected by the plate slenderness ratio but also by the other dimensional parameters such as aspect ratio, sectional area. This paper presents an experimental study on H-shaped Beams subjected to cyclic loading in large range of deformation with large depth-thickness ratios which are over or comparable with the limited values of those restricted in the current standards (Ref. [1] and [2]). The geometric parameters are relevantly identified to evaluate the plastic deformation ratio, and the new divisional rank for plastic deformation capacity of H-shaped beam is proposed.*

1 INTRODUCTION

According to the standards for steel structures in many countries, plate slenderness ratio (width-thickness ratio or depth-thickness ratio) is assumed to be of major parameter to estimate the plastic deformation capacity of thin-walled steel structures. Up to now many experimental and analytical researches have been reported aimed to reveal the relationship between plastic deformation capacity and plate slenderness ratio. These results have now been incorporated in all sorts of standard and recommendations of steel structures. Consequently, plate slenderness ratio is rigidly restrained in order to prevent the elastic buckling[1]. In Japan, the division for plate slenderness ratio of H-shaped beam is provided with respect to the plastic deformation capacity as a general provision which is only applicable in a limited region where the depth-thickness ratio is relatively small[2].

It is commonly known that coupled local buckling may dominate the H-shaped beam's behavior when the depth-thickness ratio is large. On the other hand, recent studies subjected to H-shaped Beam with large depth-thickness ratio had shown the practical use of thin plate as the earthquake-resisting element even though the plate slenderness ratio is over the limited value in some cases[2-5]. However, no standardized method is currently available for estimating the plastic deformation capacity of such beams. This paper is intended to develop an easy method to estimate the plastic deformation capacity of H-shaped beam with large depth-thickness ratio, and aims at revealing the post buckling behavior under the cyclic loading situation by contrast with those under the monotonic loading situation.

2 CYCLIC LOADING TEST

Figure 1 is the loading model subjected to the local buckling test where the lateral direction was cramped in the test arrangement so as to prevent the overall buckling. Specimens used for testing were SS400 grade, H-shaped welded steel beams. The dimension and cross-section constants for each specimen (H-D-2b-t_w-t_f), given a number is listed in Table 1, in which seven types of plates with different thickness are adopted. They are the same sort of material but a little different from each other based on the tension test due to their different thickness. The mechanical property of each plate is listed in Table 2.

Table 1: Specimens list

specimen	section(nominal value)	(surveyed value)		l
	H-D-2b-t_w-t_f	d/t_w	b/t_f	
No.1	H-350-175-3.2-12	105	7.4	1400
No.2	H-350-175-4.5-12	76	7.5	
No.3	H-350-175-4.5-16	73	5.6	
No.4	H-350-175-4.5-19	71	4.7	
No.5	H-350-175-6-9	59	10.2	
No.6	H-350-175-6-12	57	7.5	
No.7	H-350-175-6-16	56	5.6	
No.8	H-350-175-912	38	7.5	
No.9	H-350-175-4.5-12	76	7.5	1050
No.10	H-350-175-6-12	58	7.5	

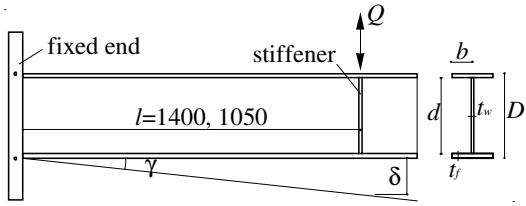

Figure 1: Loading model

Table 2: Material property

t (mm) thickness	σ_y (N/mm^2) yield stress	σ_u (N/mm^2) tensile stress	E (kN/mm^2) Yong's modulus	ε_u (%) Max strain	*Elng.* (%) fracture strain	*Y.R.* (%) yield ratio
3.2	281	424	206	19.8	29.4	66.3
4.5	267	417	205	20.9	27.8	64.0
6.0	332	433	205	17.7	29.4	76.7
9.0	291	439	206	15.0	30.4	66.3
12	306	479	205	13.0	32.6	63.9
16	266	412	209	12.3	31.8	64.6
19	257	410	206	11.8	33.1	62.7

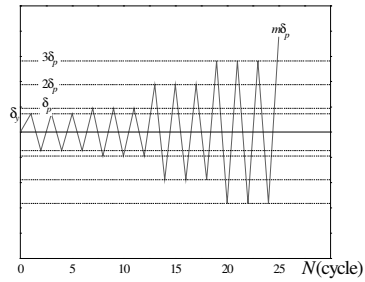

Figure 2: Loading program

Table 3: Parameter definition

marks	meaning
l	Length of beam
λ_w=l/d	Aspect ratio of web
λ_f =l/b	Aspect ratio of flange
A_w= dt_w	Sectional area of web
A_f=2bt_f	Sectional area of flange
d /t_w	Web depth-thickness ratio
b/t_f	Flange width-thickness ratio
β	Bending incline (β=1)
σ_{wy}, σ_{fy}	Yield stress of web, flange

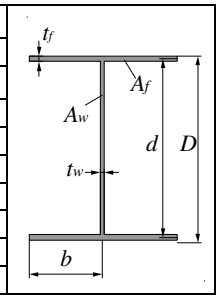

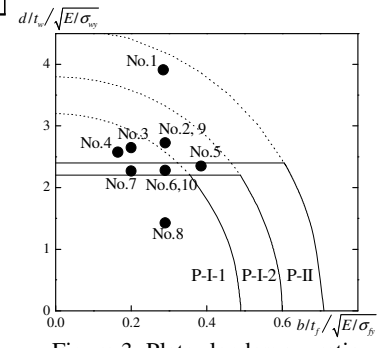

Figure 3: Plate slenderness ratio

Cyclic loading program of this test is shown in Figure 2, in which δ_y and δ_p are the displacement related with M_y And M_p given by:

$$\delta_y = \frac{M_y l^2}{3EI} + \frac{M_y}{GA_w} \tag{1}$$

$$\delta_p = \frac{M_p l^2}{3EI} + \frac{M_p}{GA_w} \tag{2}$$

In which EI and GA_w are flexural rigidity and shear rigidity. The other geometric parameters and marks used in this study are defined in Table 3. M_y And M_p denote the bending moment at the end plate on the yielded condition which can be represented by,

$$M_y = Q_y \cdot l = \frac{1}{6}\sigma_{wy} \cdot t_w (d - t_f)^2 + 2\sigma_{fy} \cdot bdt_f \tag{3}$$

$$M_p = Q_p \cdot l = \frac{1}{4}\sigma_{wy} \cdot t_w (d - t_f)^2 + 2\sigma_{fy} \cdot bdt_f \tag{4}$$

According to the Standard for Limit State Design of Steel Structures of Japan[2], the divisional curves with three ranks for width -thickness ratio and depth-thickness ratio are shown in Figure 3. The relationship between width-thickness ratio and depth-thickness ratio about each specimen is also shown by plots in the same figure.

3 EXPERIMENTAL RESULTS AND COMPARISON

3.1 Hysteresis Curve and Post Buckling Behavior

Figure 4 show the hysteresis curves of three of the specimens with different typical behaviors for No.3, No.5 and No.7 respectively. The horizontal axis and vertical axis show the dimensionless numbers for the displacement (δ) and load(Q). In the elastic region the relationship between δ and Q is defined as,

$$Q / Q_{ps} = \delta / {}_E\delta_{ps} \tag{5}$$

According to Ref.[6], Q_{ps} can be represented by,

$$\frac{Q_{ps}}{{}_wQ_p} = \begin{cases} 1 - \left[\dfrac{\sqrt{\dfrac{{}_wM_p^2}{M_p^2} - 4sb\left(1 - sb - \dfrac{{}_wM_p}{M_p}\right)} - \dfrac{{}_wM_p}{M_p}}{2sb} \right]^2 & sb > 1 - \dfrac{{}_wM_p}{M_p} \\ 1 & otherwise \end{cases} \tag{6}$$

Where, Q_{ps} denotes the yield shear load taking account of bending effect. ${}_wQ_p$ is the yield load on pure shear condition, ${}_wM_p$ denotes the full plastic moment born on web, sb denotes the ratio of shear to bending on the yield condition. They are given by,

$${}_wQ_p = A_w\sigma_{wy} / \sqrt{3} \tag{7}$$

$${}_wM_p = \frac{1}{4}t_w d^2 \sigma_{wy} \tag{8}$$

$$sb = \frac{\lambda_w / \beta}{(0.25 + A_f / A_w)\sqrt{3}} \tag{9}$$

Each hysteresis curve in Figure 4 exhibits a stable behavior until the local buckling happens. For each specimen, the load drops down immediately the local buckling happens, and a fracture is observed several cycles later, then the beam collapses in the end. As the photos of collapsed beams shown in Figure 5, the buckling modes can be divided into three typical types: (a) shows web buckling type (W.type); (b) shows coupled buckling type (C.type); (c) shows vertical buckling type (V.type). The mode of flange buckling type is not discussed due to large depth-thickness ratio of web used in this test.

Compared with the other two types, it can be observed from the Figure 4(c) that the degradation incline of V.type is extremely sharp. Vertical buckling may be induced by web local buckling when flanges are not strong enough to sustain the buckled web. As a consequence, the bending rigidity of beam quickly falls down once the buckled web makes a dent in flange. The vertical buckling does not happen even though web bucking dominates in case of Figure 4(a) because the bending burden on flange is relatively small or α(Eq.(10)) is large, hence the vertical buckling is prevented. On the other hand, the

vertical buckling does not happen in case of Figure 4(b) because the depth-thickness ratio of web is relatively small or $(d/t_w)/(b/t_f)$ is small. As a discussion result, the degradation incline of non-V.type is about -7% of the elastic incline; the necessary conditions for non-V.type are about α>0.5 or $(d/t_w)/(b/t_f)$<6 (approx).

Where, α is the ratio of shear to bending stress, equal to 0 for pure bending, can be expressed by,

$$\alpha = \left(\frac{1}{6} + \frac{A_f}{A_w}\right)\beta / \lambda_w \tag{10}$$

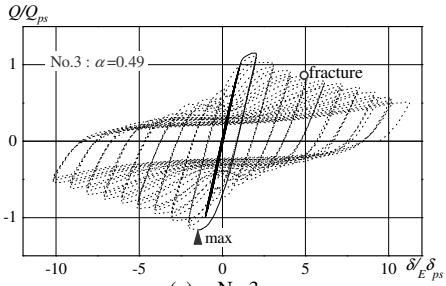

(a) No.3

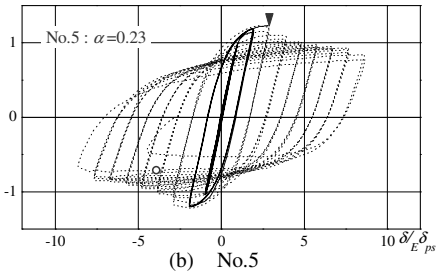

(b) No.5

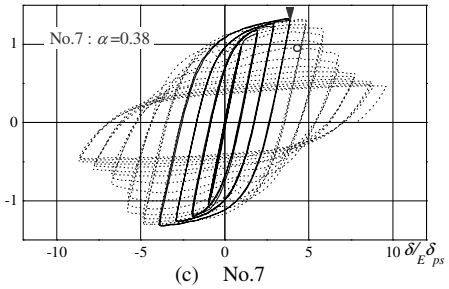

(c) No.7

Figure 4: Load- displacement hysterisis curve

(a) No.3, Web buckling type (W.type)

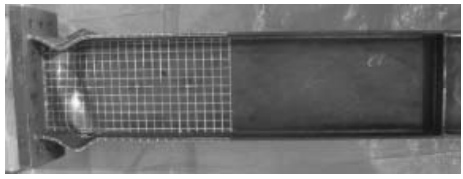

(b) No.5, Coupled buckling type (C.type)

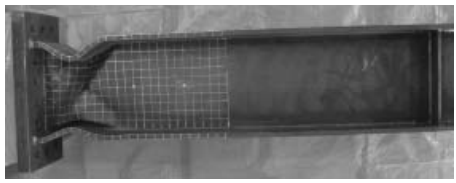

(c) No.7, Vertical buckling type (V.type)

Figure 5: Buckling mode

3.2 Skeleton curve and restriction on plate slenderness ratio

According to Ref.[7], the skeleton curve can be defined as shown in Figure 6 on the right side transformed from hysteresis curve on the left side by joining the renewed points before reaching the maximum load. After the maximum load, the skeleton curve is treated as wrapping line.

Based on the rule defined in Figure 6, all hysteresis curves of the specimens (appendix Figure A) are transformed into the skeleton curves (Figure 7). The maximum load of No.2 and No.3 shown in Figure 7

are over the plastic shear load Q_{ps} even though their depth-thickness ratios are lager than the limited values, indicating that the restriction for depth-thickness ratio in Ref. [1] and [2] is conservative.

According to Ref.[5], improved method for restriction of width (depth)-thickness ratio had been proposed. The restriction curve is expressed as follows:

$$\left(\frac{BTW}{BTW0}\right)^3+\left[4.63-125\left(\frac{\sqrt{E/\sigma_{wy}}}{BTW0}\right)^3\right]\left(\frac{BTF}{\sqrt{E/\sigma_{fy}}}\right)^3=1 \tag{11}$$

Where, α is given as Eq. (10), $BTW0$ is given by Eq. (12) below:

$$\frac{BTW0}{\sqrt{E/\sigma_{wy}}}=\begin{cases}4.9 & \alpha<1/6\\ 5.75-5.1\alpha & 1/6\le\alpha\le 1/2\\ 3.2 & \alpha>1/2\end{cases} \tag{12}$$

BTW and *BTF* are the restrictive value of depth and width-thickness ratio. They are proposed by taking account of the effect of plate slenderness ratio and the other geometric parameters comprising plate sectional area and aspect ratio based on the calculation of buckling strength.

As a sample shown in Figure 8 where the rectangular plots are the value on restriction curves obtained from Eq. (11), circle plots are the real width (depth)-thickness ratio of each beam, the ratio of the value at circle plots to rectangular plots on each situation can be represented by,

$$WF=\frac{d/t_w}{BTW}=\frac{b/t_f}{BTF} \tag{13}$$

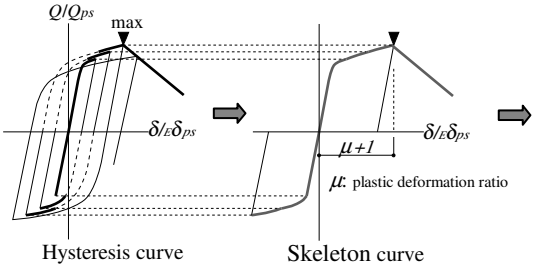

Figure 6: Definition of skeleton curve

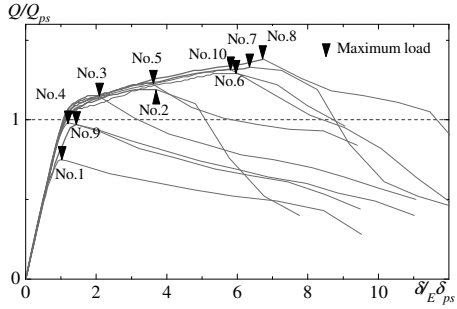

Figure 7: Skeleton curves (all specimens)

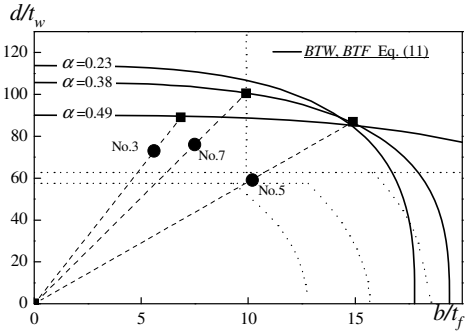

Figure 8: Restriction curve (Eq. (11))

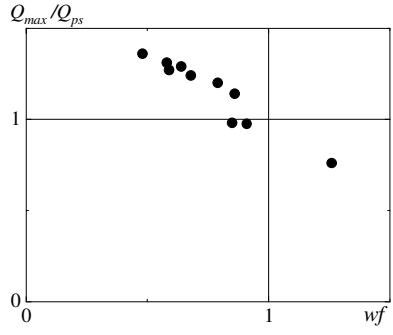

Figure 9: Maximum load and *wf*

Where, *WF* is referred to as normalized plate slenderness ratio.
Substituting form Eq. (11) into Eq. (13), *WF* is given by,

$$WF = \left[\frac{(d/t_w)^3}{BTW0^3} + \frac{4.63(b/t_f)^3}{(E/\sigma_{fy})^{3/2}} - \frac{125(b/t_f)^3}{BTW0^3} \right]^{1/3} \tag{14}$$

Figure 9 shows the relationship between *WF* and maximum load Q_{max}. It can be observed from the figure that $Q_{max} > Q_{ps}$ when *WF*<1. Therefore, the normalized plate slenderness ratio *WF* defined in Eq.(14) can be regarded as a parameter to restrict the beam dimension to prevent elastic local buckling.

4 PLASTIC DEFORMATION RATIO AND NORMALIZED SLENDERNESS RATIO

In Figure 6, μ denotes the plastic deformation ratio at the point of maximum load, it is a parameter defined to evaluate the plastic deformation capacity in this study. As shown in Figure 3, the divisional curve of P-I-1 is to ensure μ>4, P-I-2 is to ensure μ>2, P-II is to ensure μ>0 and $Q_{max} > Q_{ps}$.

Figure 10(b) and (c) show the relationship between *WF* and μ obtained from a number of FEM analysis subjected to monotonic loading where the same models as Figure 1 was adopted. The width-thickness and depth-thickness ratio about each beam is shown in Figure 10(a). The aspect ratio of web of each beam is set at $2<\lambda_w=l/d<12$. According to the buckling modes, the results are roughly divided into two parts in Figure 10(a). Figure 10(b) shows the plots in case of $(d/t_w)/(b/t_f)$ <3, or $(d/t_w)/(b/t_f)$>6 where a large part of their buckling modes are single buckling modes or non-C.type buckling modes. Figure 10(c) shows the plots in case of $3<(d/t_w)/(b/t_f)<6$ which are assumed to be the coupled buckling modes. According to the plots showing the relationship between *WF* and μ in both Figure 10(b) and (c), μ tends to become larger as *WF* becomes smaller. Therefore, *WF* can be reasonably regarded as a major parameter to estimate the plastic deformation ratio.

As described earlier (Chapter 3.1), the load falls down immediately after the buckling, such phenomenon is independent to the buckling style in case of cyclic loading situation. But the load does not fall down immediately after the single buckling in case of monotonic loading situation. Consequently, there is some dispersion in the Figure 10(b). But the dispersion in Figure 10(c) is small due to its coupled buckling modes.

To minimize the dispersion and evaluate the plastic deformation capacity safely, the normalized slenderness ratio *WF* expressed by Eq. (14) is modified as *wf* given by

$$wf = \sqrt{\frac{(d/t_w)^2}{BTW0^2} + \left(\frac{5\sigma_{fy}}{E} - \frac{36}{BTW0^2} \cdot \frac{\sigma_{fy}}{\sigma_{wy}} \right) (b/t_f)^2} \tag{15}$$

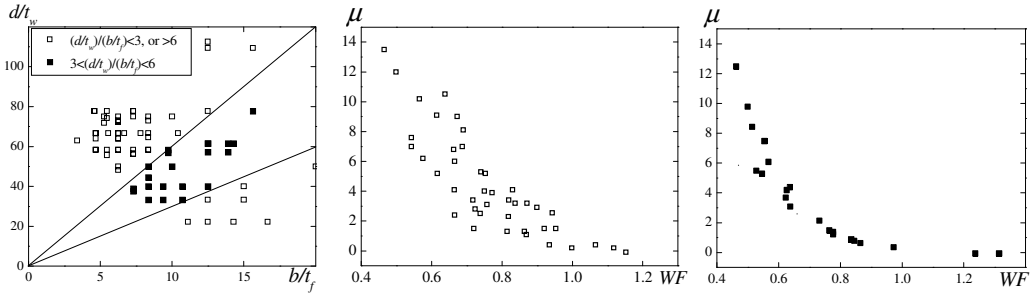

(a): Object of depth and width-thickness ratio (b): $(d/t_w)/(b/t_f)$ <3 or >6 (c): $3<(d/t_w)/(b/t_f)<6$

Figure 10: Plastic deformation capacity and *wf*

Where, α is given as Eq. (10), $BTW0$ is given as Eq. (16).

$$\frac{BTW0}{\sqrt{E/\sigma_{wy}}} = \begin{cases} 4.4 & \alpha < 1/6 \\ 5.18 - 4.6\alpha & 1/6 \le \alpha \le 1/2 \\ 2.9 & \alpha > 1/2 \end{cases} \tag{16}$$

Figure 11(a) shows the relationship between μ and wf (Eq. (15)). Each black plot denotes the case when plate slenderness ratio is over the restricted value as shown in Figure 11(b). According to the position of these black plots in Figure 11(a), the restriction can be alleviated in case of wf<1. The circle plots denoting the results under cyclic loading in this test are smaller than the other cases. They are distributed in the lower limit. To estimate the plastic deformation capacity reasonably, the lower limit of μ must be adopted due to the disadvantageous loading situation. According to the result shown in Figure 11, the divisional rank for plastic deformation capacity is proposed as follows:

Rank P-I-1(μ>4): wf<0.75;

Rank P-I-2(μ>2): wf<0.85;

Rank P-II (μ>0): wf<1.

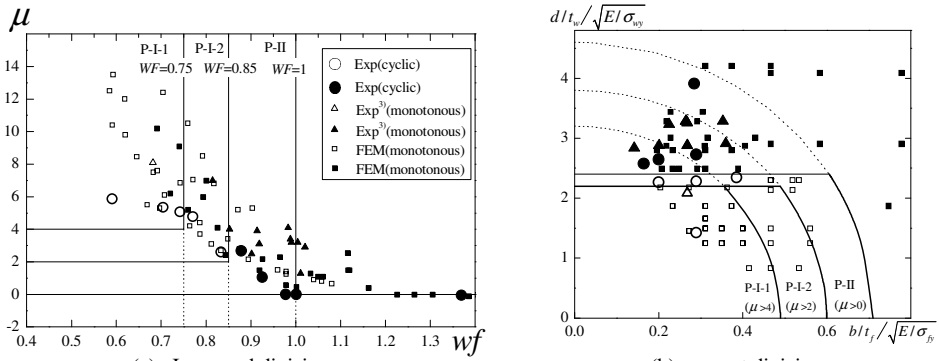

(a): Improved division (b): current division

Figure 11: Division for plastic deformation capacity

5 CONCLUSIONS

This paper presents an experimental study of the local buckling behavior subjected to H-shaped beam. The current standards for steel structures (ref.[1] and [2]) are shown to be generally conservative. According to the hysteresis curve of each specimen, the vertical buckling induced by web local buckling was found to be the major effect on the deterioration. The approximation of the necessary conditions for non-vertical buckling type was given. Compared with experiment and a number of numerical analysis under monotonic loading situation, the plastic deformation ratio of the beams under cyclic loading is relatively small in case of beam with non-C.type buckling modes. The geometrical parameters such as aspect ratio, sectional area as well as the plate slenderness ratio are identified to evaluate the plastic deformation ratio. Improved division for plastic deformation capacity is proposed using normalized plate slenderness ratio.

REFERENCES:

[1] Architectural institute of Japan, “Design Standard for Steel Structures”, 2005.

[2] Architectural institute of Japan “Standard for Limit State Design of Steel Structures”, 2002.

[3] Toshiro SUZUKI, Kikuo IKARASHI and Yasuhiro TSUNEKI, “A Study on Collapse Mode and Plastic Deformation Capacity of H-Shaped Steel Beams under Shear Bending”, *Journal of Structural and Construction Engineering, Arch, inst. of Japan,* No.547, 185-191, 2001 .9

[4] Kikuo IKARASHI and Tao WANG, "A Method for Evaluation of Elastic Buckling Strength of H-Shaped Steel Member under Bending-Shear and Axial Force", *Journal of Structural and Construction Engineering, Arch, inst. of Japan,* No.613, 137-146, 2007.3

[5] Kikuo IKARASHI and Tao WANG, "Evaluation of Width-Thickness Ratio Limitation of H-Shaped Beam Members Based on Coupled Buckling Analysis", *Journal of Structural and Construction Engineering, Arch, inst. of Japan,* No.629, 1177-1184, 2008.7

[6] Japan Society of Civil Engineers, "Guidelines for Stability Design Steel Structures", 2005.

[7] Architectural institute of Japan, "Evaluation Procedures for Performance -Based Seismic Design of Buildings -Calculation of Response and Limit Strength, Energy Balance -Based Seismic Resistant Design, Time History Response Analysis- ", 2009.2

APPENDIX:

Table A: Test result

Specimen	No.1	No.2	No.3	No.4	No.5	No.6	No.7	No.8	No.9	No.10
α	0.51	0.38	0.49	0.57	0.23	0.30	0.38	0.21	0.50	0.40
WF	1.37	0.88	0.93	0.98	0.83	0.74	0.7	0.59	1	0.77
μ	0	2.67	1.05	0	2.55	5.07	5.45	5.86	0	4.78
Buckling mode	W	V	W	W	C	V	V	C	W	C

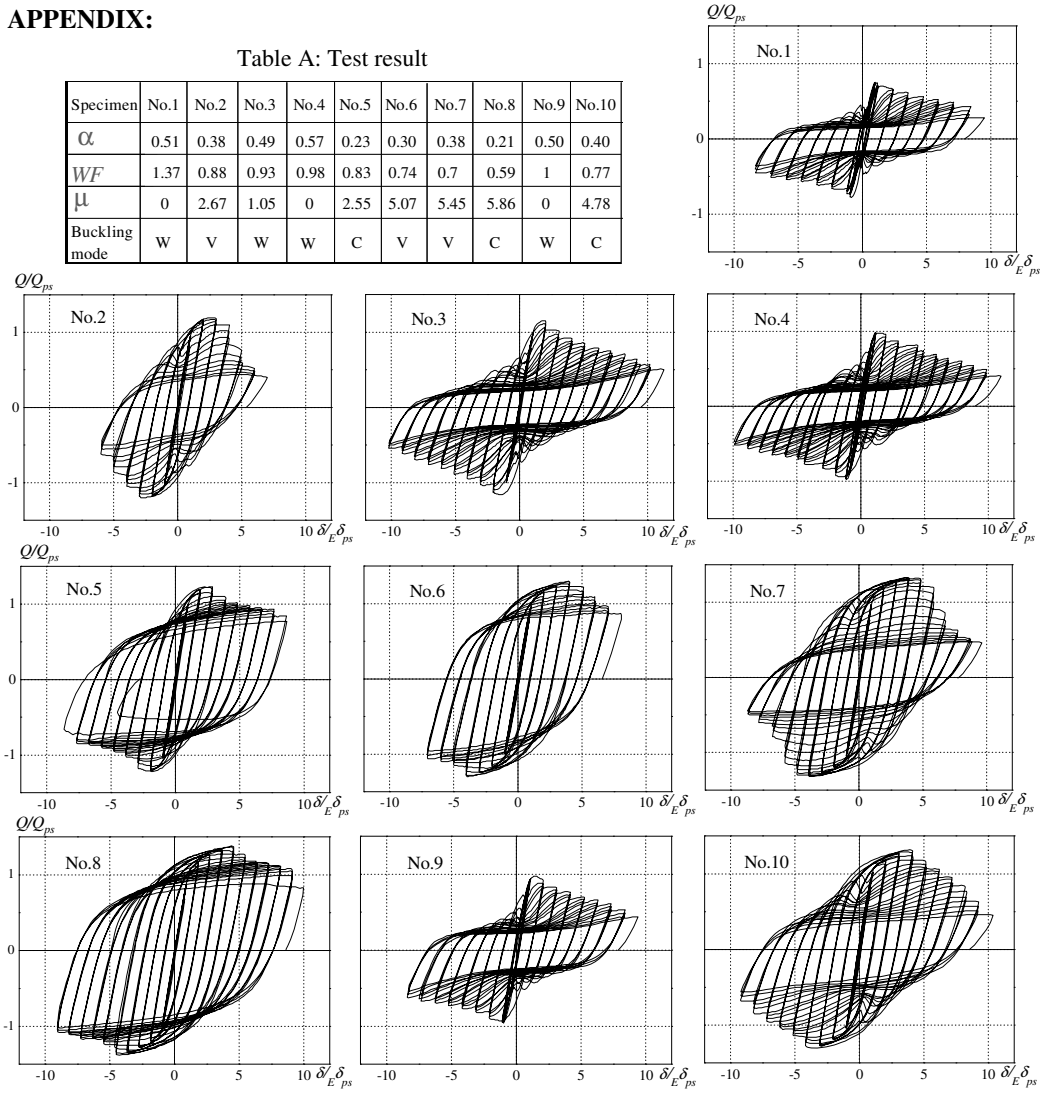

Figure A: Hysteresis curves (all specimens)